NASA Contractor Report 3148

High Energy Proton Radiation Damage to (AlGa)As—GaAs Solar Cells

R. Loo, L. Goldhammer,
S. Kamath, and R. C. Knechtli

CONTRACT NAS1-14727
JUNE 1979

NASA

NASA Contractor Report 3148

High Energy Proton Radiation Damage to (AlGa)As—GaAs Solar Cells

R. Loo, L. Goldhammer,
S. Kamath, and R. C. Knechtli
Hughes Research Laboratories
Malibu, California

Prepared for
Langley Research Center
under Contract NAS1-14727

NASA
National Aeronautics
and Space Administration

Scientific and Technical
Information Office

1979

TABLE OF CONTENTS

LIST OF ILLUSTRATIONS

SECTION 1

INTRODUCTION AND SUMMARY

The objective of this contract was to measure the radiation damage produced by high-energy proton irradiation on representative (AlGa)As-GaAs solar cells, and to compare it to the damage produced on Si solar cells under the same conditions. Toward this end, twelve 2 x 2 cm^2 (AlGa)As-GaAs solar cells and several representative silicon cells were irradiated with 15.4 MeV and 40 MeV protons at fluences of 5 x 10^{10} and 5 x 10^{11} P/cm^2 (see Appendix A). The full matrix of tests performed is given in Table 1.

Table 1. High-Energy Proton Irradiation Specification

Proton Energy, MeV	Proton Fluence, P/cm^2	Type and Number of Cells		
		(AlGa)As-GaAs[a]	K7[b]	Conventional[c]
15.4	5 x 10^{10}	3	5	4
15.4	5 x 10^{11}	3	4	4
40	5 x 10^{10}	3	2	3
40	5 x 10^{11}	3	2	3

[a] cell size = 2 x 2 cm^2.

[b] n on p, 0.3 μm junction depth 2.1 x 2.0 cm^2, 11 mils thick, 10 Ω-cm, back surface field high efficiency silicon solar cells with Ta_2O_5 antireflection coating (no cover glass).

[c] n on p, 0.3 μm junction depth, 2.0 x 2.0 cm^2, 12 mils thick high efficiency silicon solar cells with SiO_x antireflection coating (no cover glass).

Figure 1 shows the baseline structure of the solar cell used. (AlGa)As window layer and the depth of the junction were each kept below 0.5 μm; a GaAs buffer layer ≈20 μm thick was grown to minimize the effects of variations in substrate properties. No cover glass was applied to these cells.

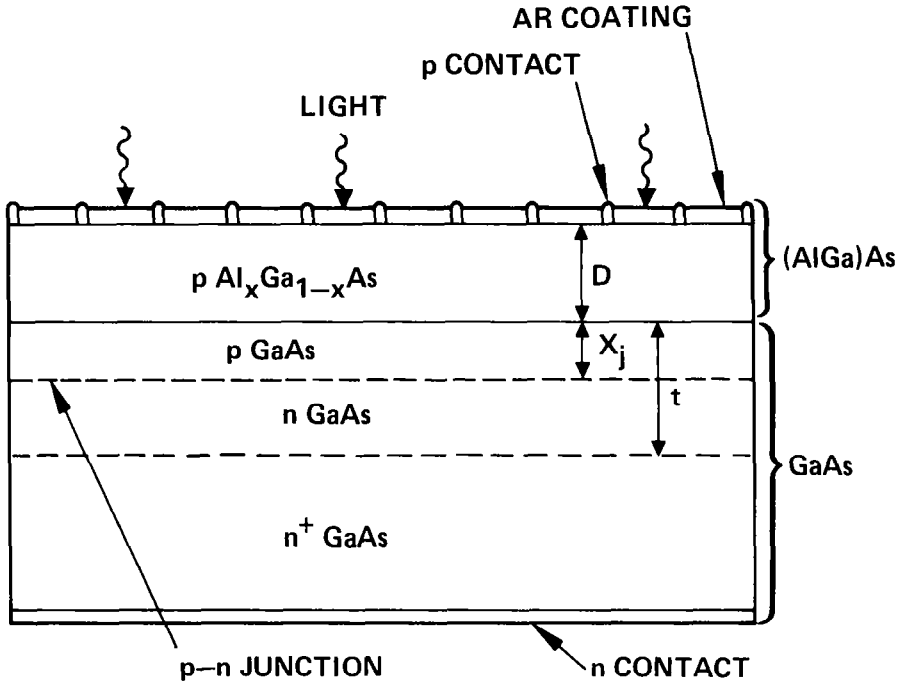

p = 10^{18} cm^{-3} (Be)

n = 10^{17} cm^{-3} (Sn)

n^+ = 10^{18} cm^{-3} (Te)

D $< 0.5\ \mu m$

$X_j \leqslant 0.5\ \mu m$

t $> 20\ \mu m$

NUMBER OF FINGERS = 24

p CONTACT: Au–Zn–Ag

n CONTACT: Au–Ge–Ni–Ag

AR COATING: Ta_2O_x

p $Al_xGa_{1-x}As$: $x \geqslant 0.95$

CELL SIZE = 2 x 2 cm^2

Figure 1. Parameters of the (AlGa)As-GaAs solar cell used for proton damage.

High-energy proton irradiation was performed at the Crocker Nuclear Laboratory at the University of California at Davis. This cyclotron can produce a primary proton beam at energies between approximately 8 and 68 MeV. The solar cells were mounted with small pieces of double-face masking tape to aluminum plates. Each plate was irradiated separately in air at specific proton energies and fluences*. The fluence over the target plane was uniform within ±5%. The cell temperature during irradiation was kept at 30°C

The results of these proton irradiation tests are summarized in Figures 2 and 3, which show the maximum solar cell output power versus proton irradiation fluence for the three types of cells specified in Table 1. Figure 2 shows the tests for 15.4 MeV proton irradiation, and Figure 3 shows the tests with 40 MeV protons. The (AlGa)As-GaAs solar cells are substantially more resistant to high-energy proton radiation damage than are any of the silicon cells. In addition to these test results, the dotted lines plotted in Figures 2 and 3 are an extrapolation of our test results; these show the effect expected from proton fluence on an improved (AlGa)As-GaAs solar cell with a beginning-of-life power-conversion efficiency of 18%. This extrapolation is pertinent since the feasibility of an 18% efficiency has already been demonstrated for this type of cell.**

More detailed data and observations on the tests of the (AlGa)As cells are given in the following sections. Similar data for the Si cells are given in Appendix B.

---

*By comparing the results from the previous irradiated solar cells both in air and in vacuum, Lee Goldhammer has found that the ionized gases in air surrounding the cell during irradiation have no effect on the cell.

**H.J. Hovel and J.M. Woodall, "Improved GaAs solar cells with very thin junctions," 12th IEEE Photovoltaic Specialists Conference, 1976, pp. 945-947.

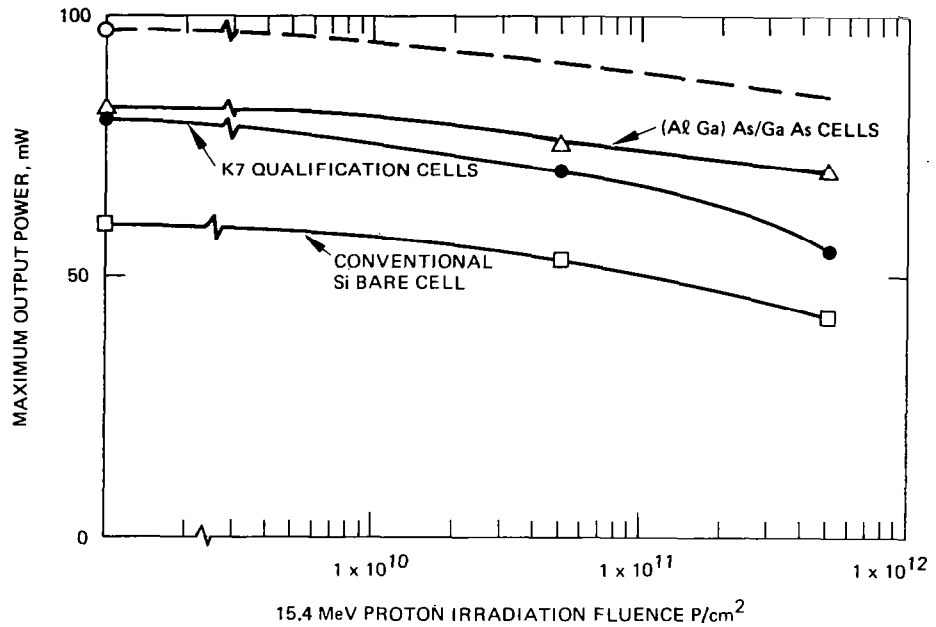

Figure 2. Solar cell maximum output power versus 15.4 MeV proton irradiation fluence.

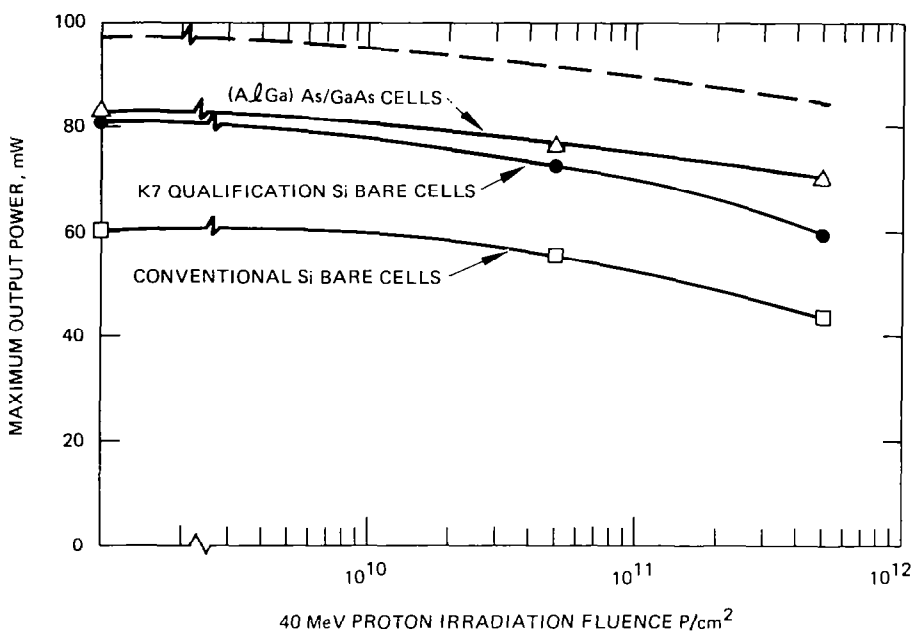

Figure 3. Solar cell maximum output power versus 40 MeV proton irradiation fluence.

SECTION 2

PHOTO CURRENT-VOLTAGE CHARACTERISTICS

The high-energy proton irradiation test matrix for the (AlGa)As-GaAs solar cells is given in Table 2.

Table 2. Proton Irradiation Test Matrix for the (AlGa)As-GaAs Solar Cells

Proton Energy, MeV	Proton Fluence, P/cm^2	(AlGa)As-GaAs Solar Cells[a]
15.4	5×10^{10}	Cell No. 1012; 1069; 1087
15.4	5×10^{11}	Cell No. 1052; 1138; 1078
40	5×10^{10}	Cell No. 1068; 1076; 1096
40	5×10^{11}	Cell No. 1075; 1090; 1136

[a](AlGa)As-GaAs solar cells without cover glass.

Figures 4 through 15 show the Air Mass 0 (AM0) photo current-voltage (I-V) characteristics before and after irradiation for these 12 (AlGa)As-GaAs solar cells. Table 3 gives the following characteristics of the individual cells for both before and after irradiation: short circuit current (I_{sc}), open circuit voltage (V_{oc}), fill factor (FF), maximum output power (P_{max}), and power conversion efficiency. A study of the trends of these measured values reveals several interesting generalizations:

- 15.4 MeV and 40 MeV energies of protons cause approximately the same amount of damage to the (AlGa)As-GaAs solar cells.
- The (AlGa)As-GaAs solar cells see only a moderate amount of degradation at 15.4 MeV and 40 MeV proton energies at both the fluences studied (5×10^{10} and 5×10^{11} P/cm^2).

Table 3. Electrical Characteristics of (AlGa)As/GaAs Solar Cells Before and After Proton Irradiation

Cell Number	Proton MeV	Fluence Level, p/cm^2	I_{sco}, mA	V_{oc}, V	FF_o *	P_{max}, mW	η_o, %	$\frac{\Delta I_{sc}}{I_{sco}}$, %	$\frac{\Delta \eta}{\eta_o}$, %
1012	0	0	107	1.01	0.753	81.34	15.1		
	15.4	5×10^{10}	102.5	0.995	0.744	75.85	14.0	4.2	7.9
1069	0	0	106	1.01	0.78	82.65	15.3		
	15.4	5×10^{10}	102	1.0	0.748	76.36	14.1	3.8	7.8
1087	0	0	106	1.0	0.762	80.75	14.9		
	15.4	5×10^{10}	102	0.98	0.745	74.52	13.8	3.8	7.4
1052	0	0	112	1.0	0.75	84	15.5		
	15.4	5×10^{11}	97	0.95	0.727	66.99	12.37	13.4	20.2
1138	0	0	108.5	1.02	0.757	83.725	15.45		
	15.4	5×10^{11}	98	0.97	0.754	71.69	13.24	10.5	14.3
1078	0	0	111.5	1.0	0.735	82.0	15.1		
	15.4	5×10^{11}	99.5	0.94	0.68	63.9	11.8	10.8	21.8
1068	0	0	107.5	1.02	0.745	81.7	15.1		
	40	5×10^{10}	105	1.0	0.73	76.73	14.2	2.3	6.0
1076	0	0	112	1.01	0.748	83.73	15.5		
	40	5×10^{10}	109	1.0	0.705	76.8	14.2	2.7	8.4
1096	0	0	107	1.01	0.771	82.56	15.24		
	40	5×10^{10}	103	1.0	0.753	77.61	14.33	3.7	5.9
1075	0	0	109	1.0	0.773	84.28	15.6		
	40	5×10^{11}	100	0.97	0.755	73.26	13.5	8.25	13.5
1090	0	0	110	0.99	0.738	80.36	14.83		
	40	5×10^{11}	103.5	0.93	0.65	62.56	11.55	5.9	22.1
1136	0	0	105	1.01	0.77	82.03	15.1		
	40	5×10^{11}	99	0.97	0.75	72.45	13.38	5.7	11.4

*The change in fill factor after irradiation is caused by the degradation in the space charge region.

- The three cells irradiated at 15.4 MeV (5×10^{11} P/cm^{-2}) and the three irradiated at 40 MeV (5×10^{11} P/cm^{-2}) degrade at different rates. Although the reason for this variation is not clear, it does indicate that the cells can be optimized to minimize the degradation to the lowest levels observed. Even the worst cell is considerably superior to the best silicon cell. (See Figures 2 and 3.)

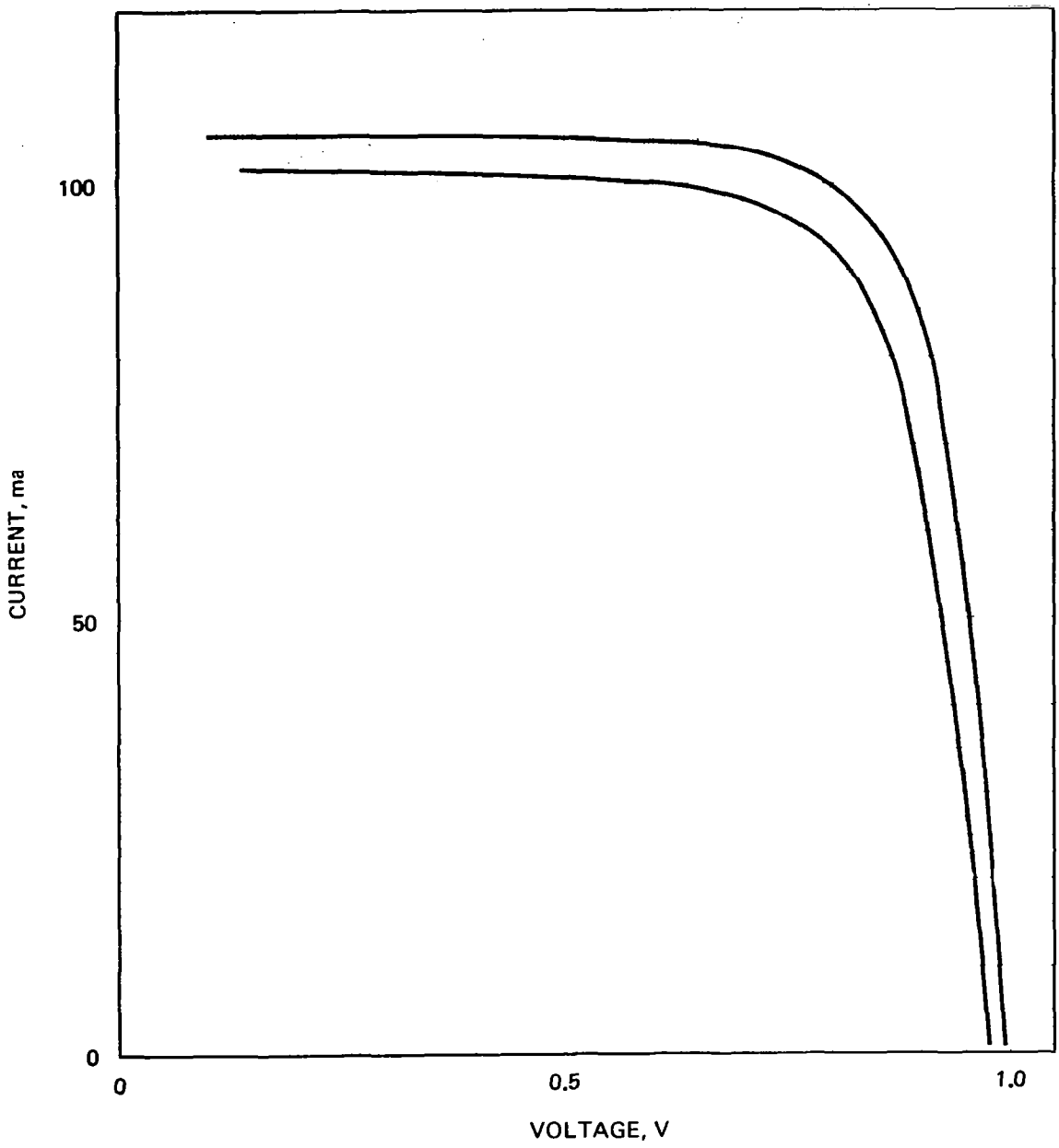

Figure 4. Photo I-V characteristics before and after proton irradiation, 15.4 MeV, 5 x 10^{10} P/cm^2, cell No. 1087.

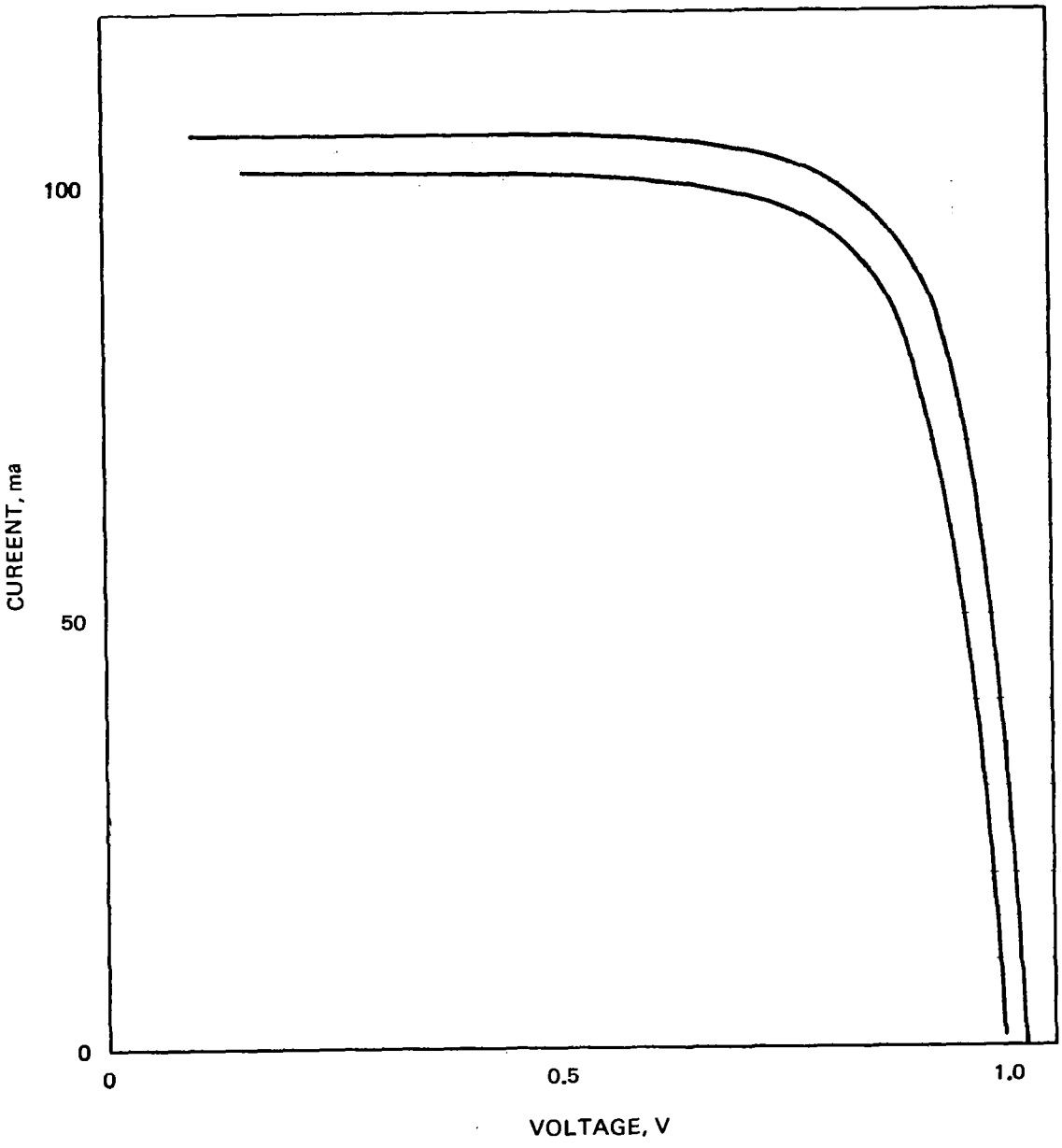

Figure 5. Photo I-V characteristics before and after proton irradiation, 15.4 MeV, 5 x 10^{10} P/cm^2, cell No. 1069.

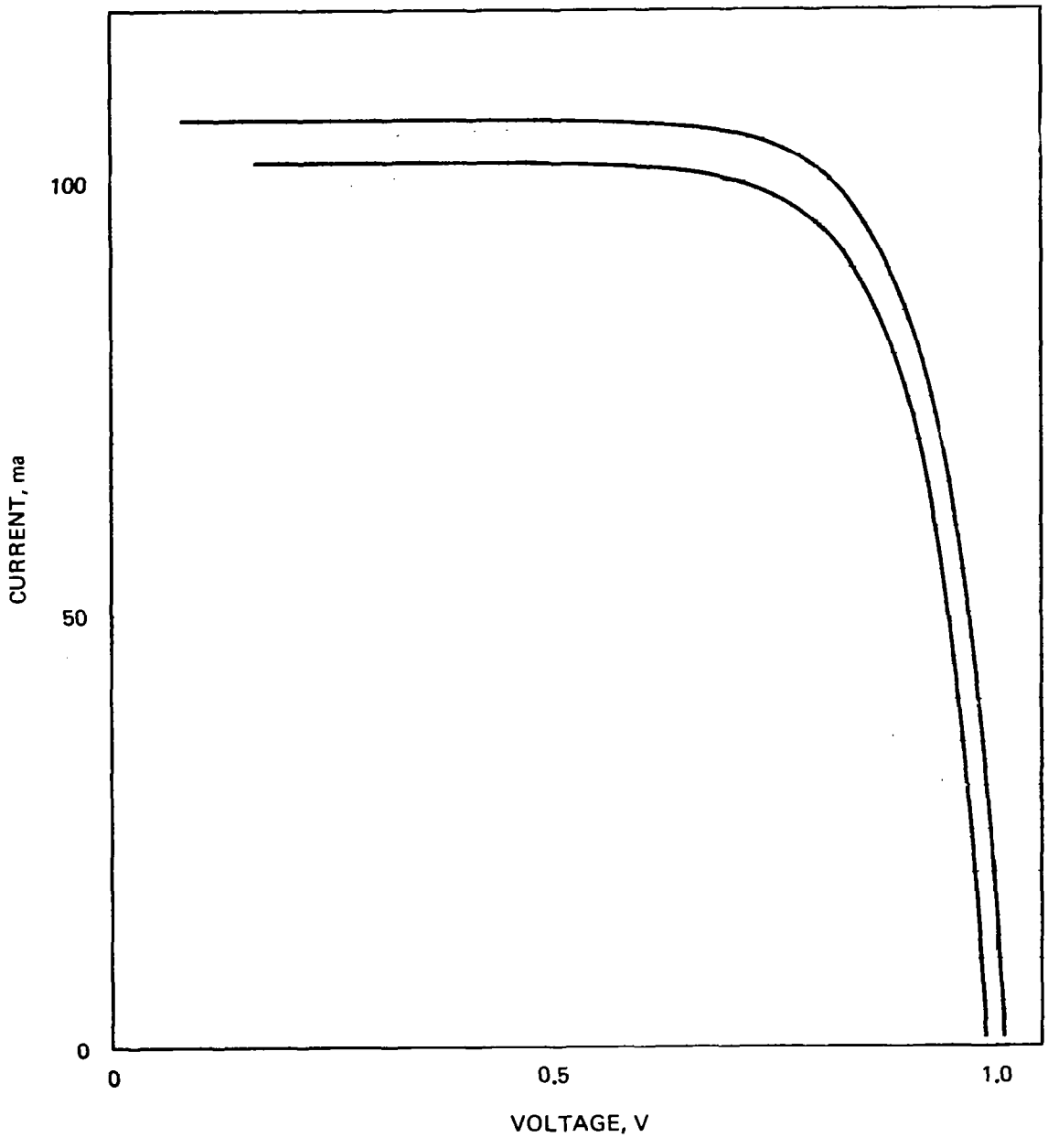

Figure 6. Photo I-V characteristics before and after proton irradiation, 15.4 MeV, 5 x 10^{10} P/cm^2, Cell No. 1012.

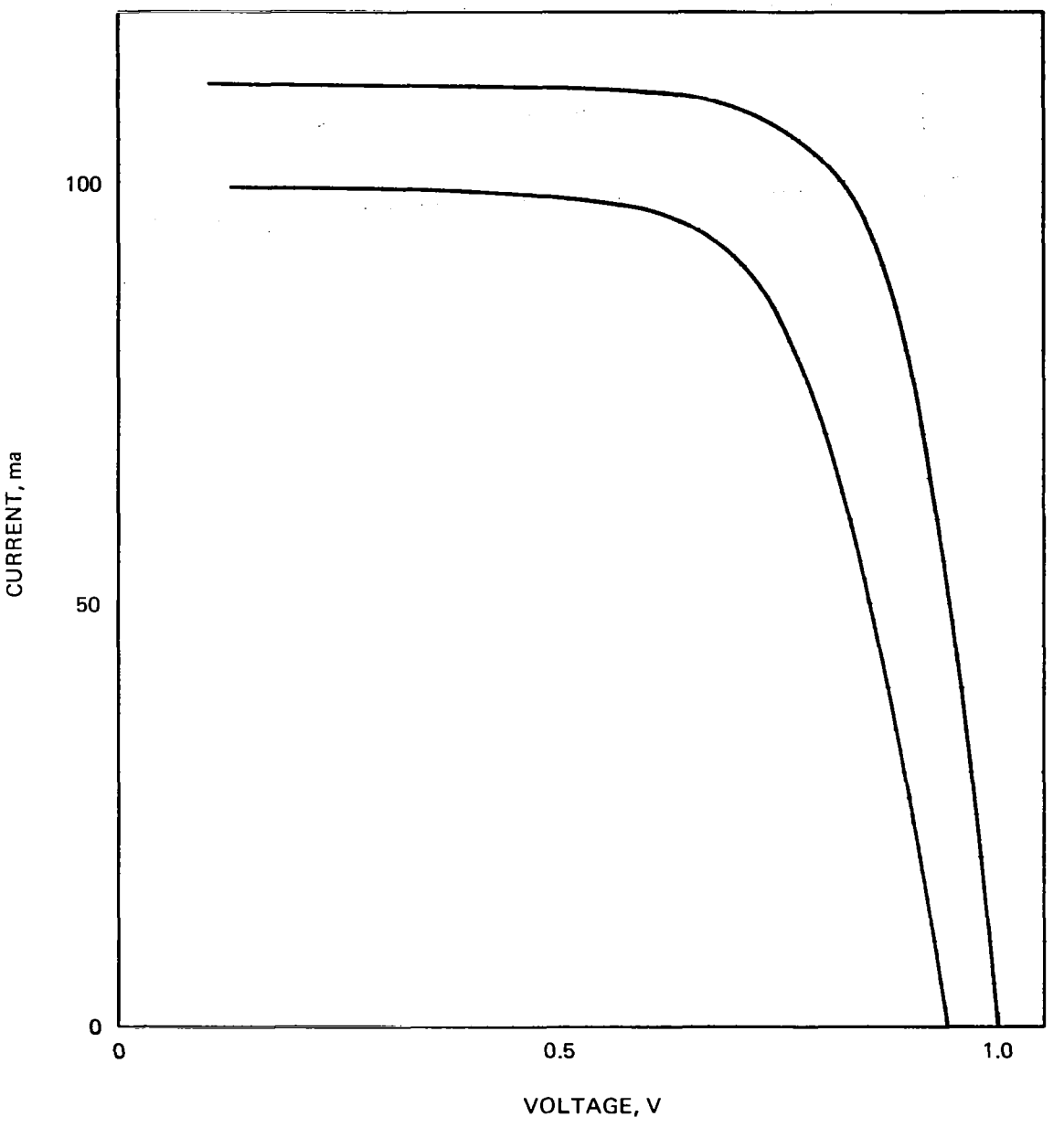

Figure 7. Photo I-V characteristics before and after proton irradiation, 15.4 MeV, 5 x 10^{11} P/cm^2, Cell No. 1078.

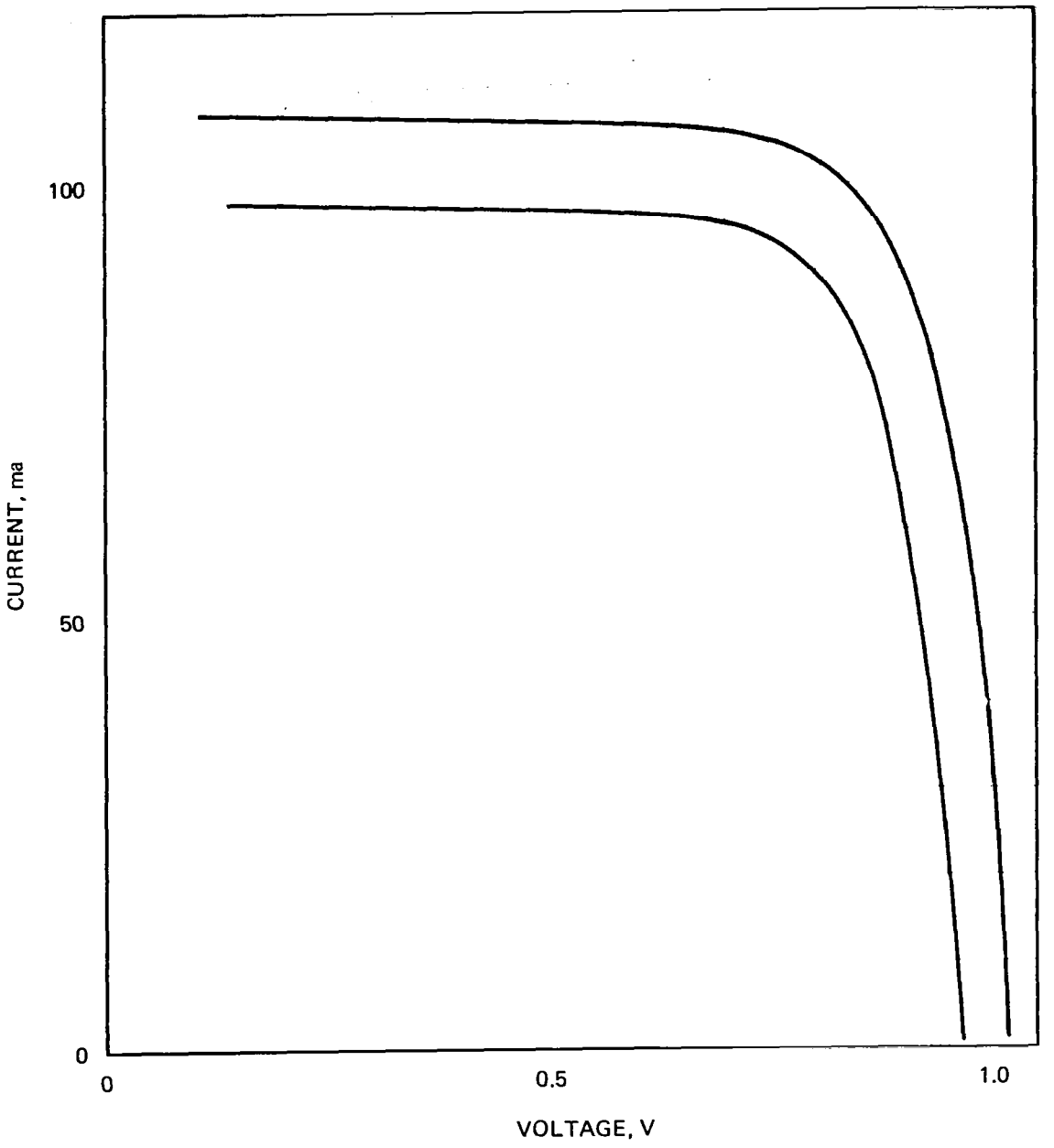

Figure 8. Photo I-V characteristics before and after proton irradiation, 15.4 MeV, 5 x 10^{11} P/cm^2, Cell No. 1138.

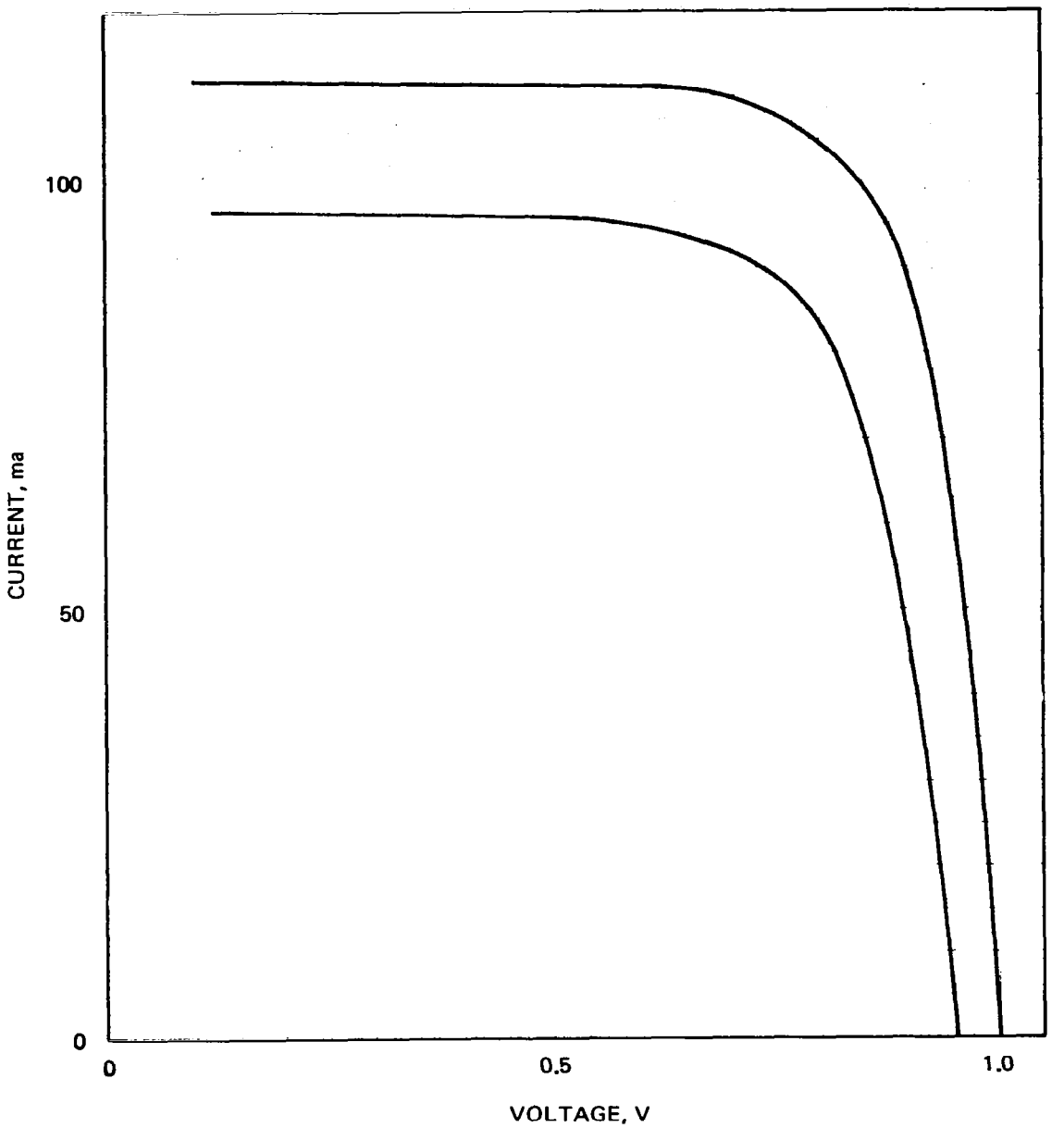

Figure 9. Photo I-V characteristics before and after proton irradiation, 15.4 MeV, 5 x 10^{11} P/cm^2, Cell No. 1052.

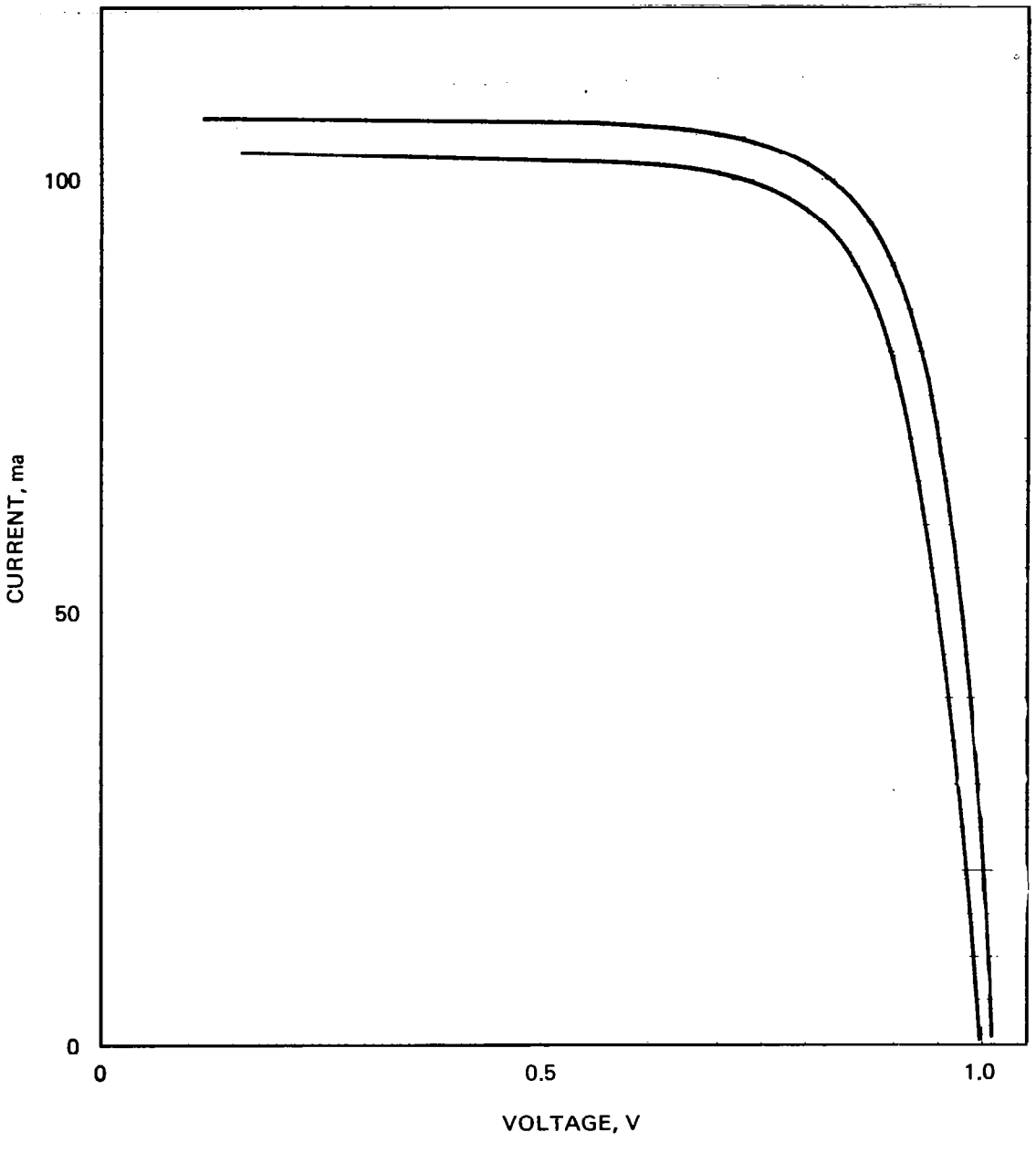

Figure 10. Characteristics before and after proton irradiation, 40 MeV, 5 x 10^{10} P/cm^2, Cell No. 1096.

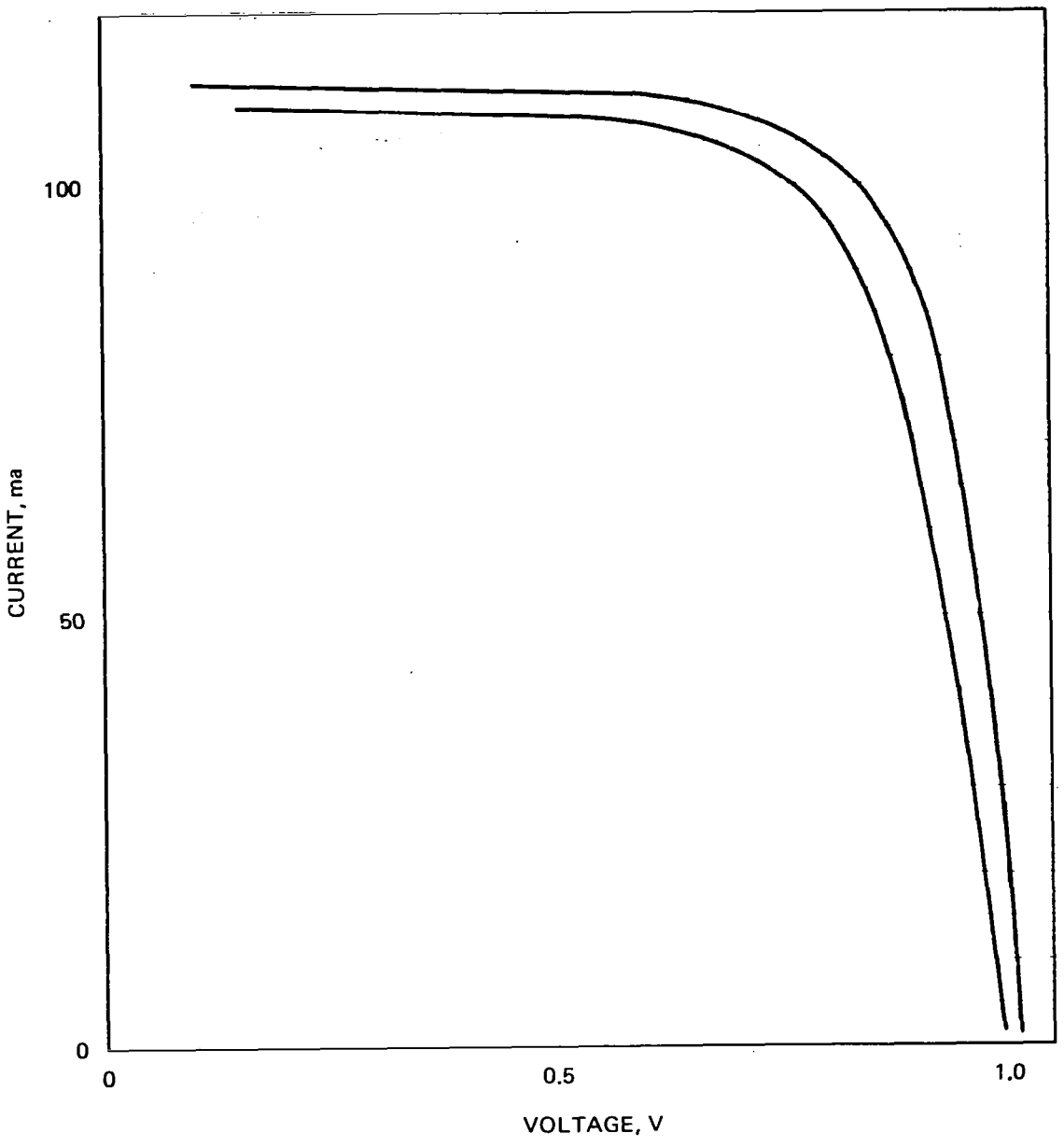

Figure 11. Photo I-V characteristics before and after proton irradiation, 40 MeV, 5 x 10^{10} P/cm^2, Cell No. 1076.

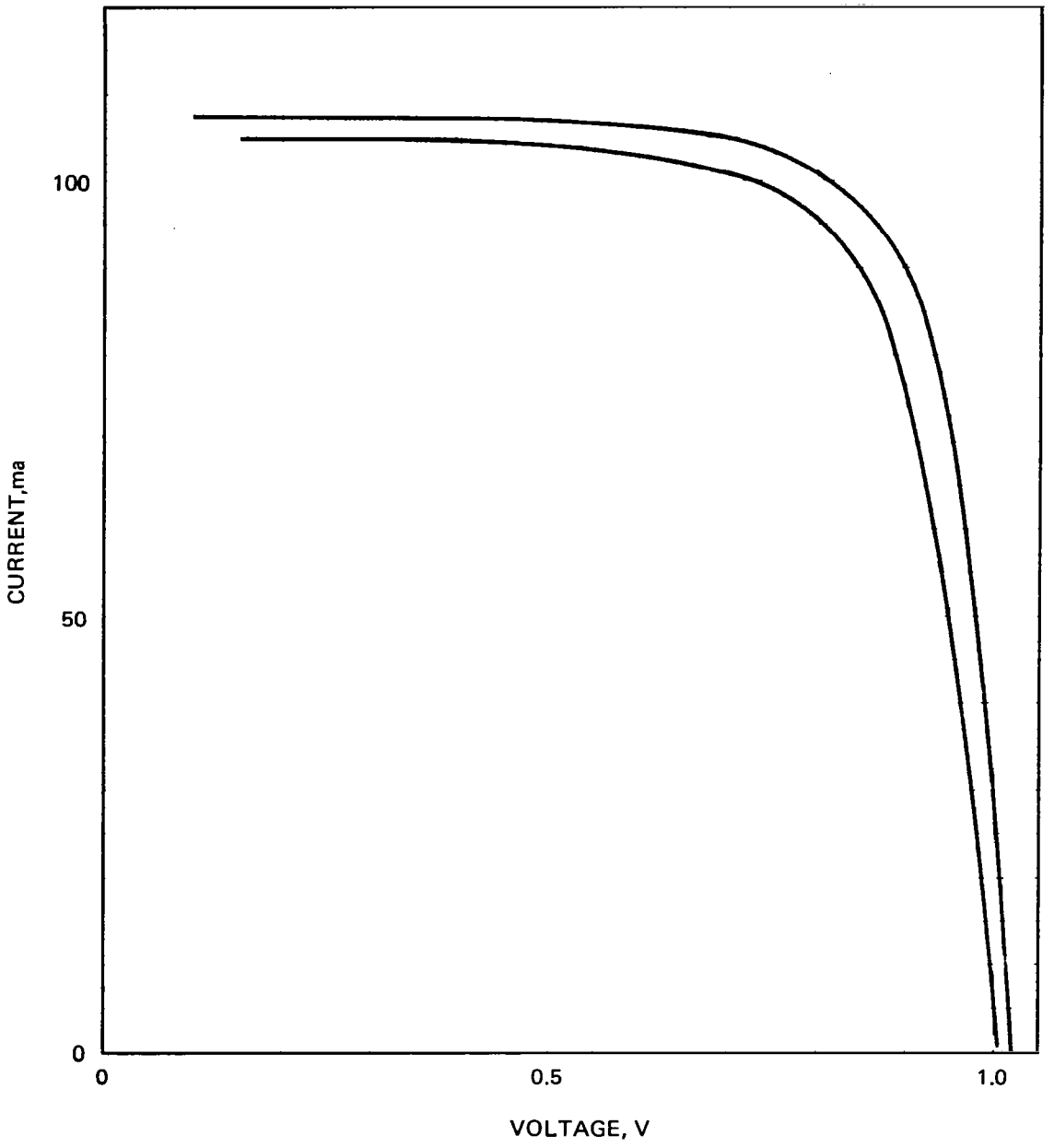

Figure 12. Photo I-V characteristics before and after proton irradiation, 40 MeV, 5 x 10^{10} P/cm^2, Cell No. 1068.

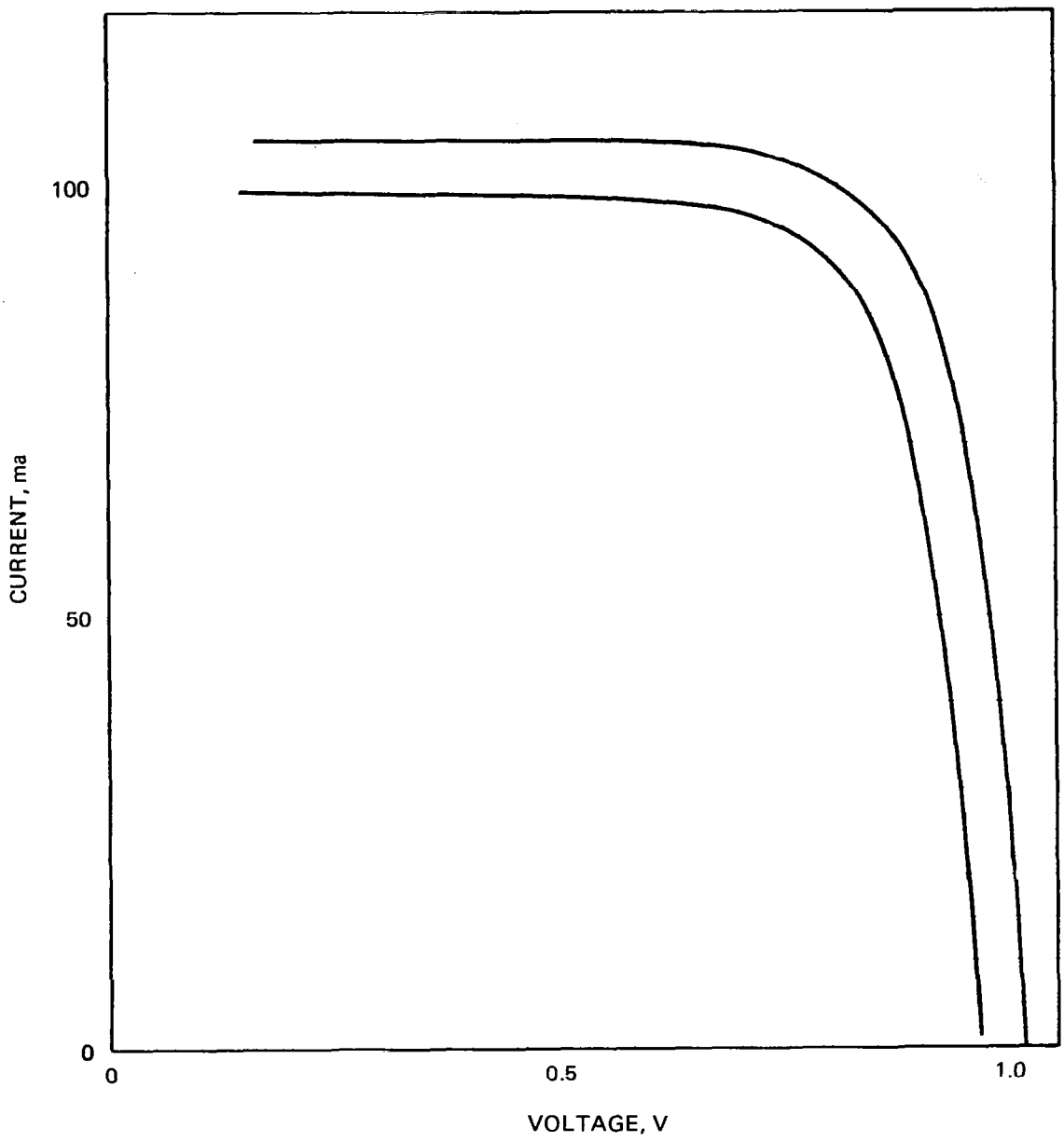

Figure 13. Photo I-V characteristics before and after proton irradiation, 40 MeV, 5 x 10^{11} P/cm^2, Cell No. 1136.

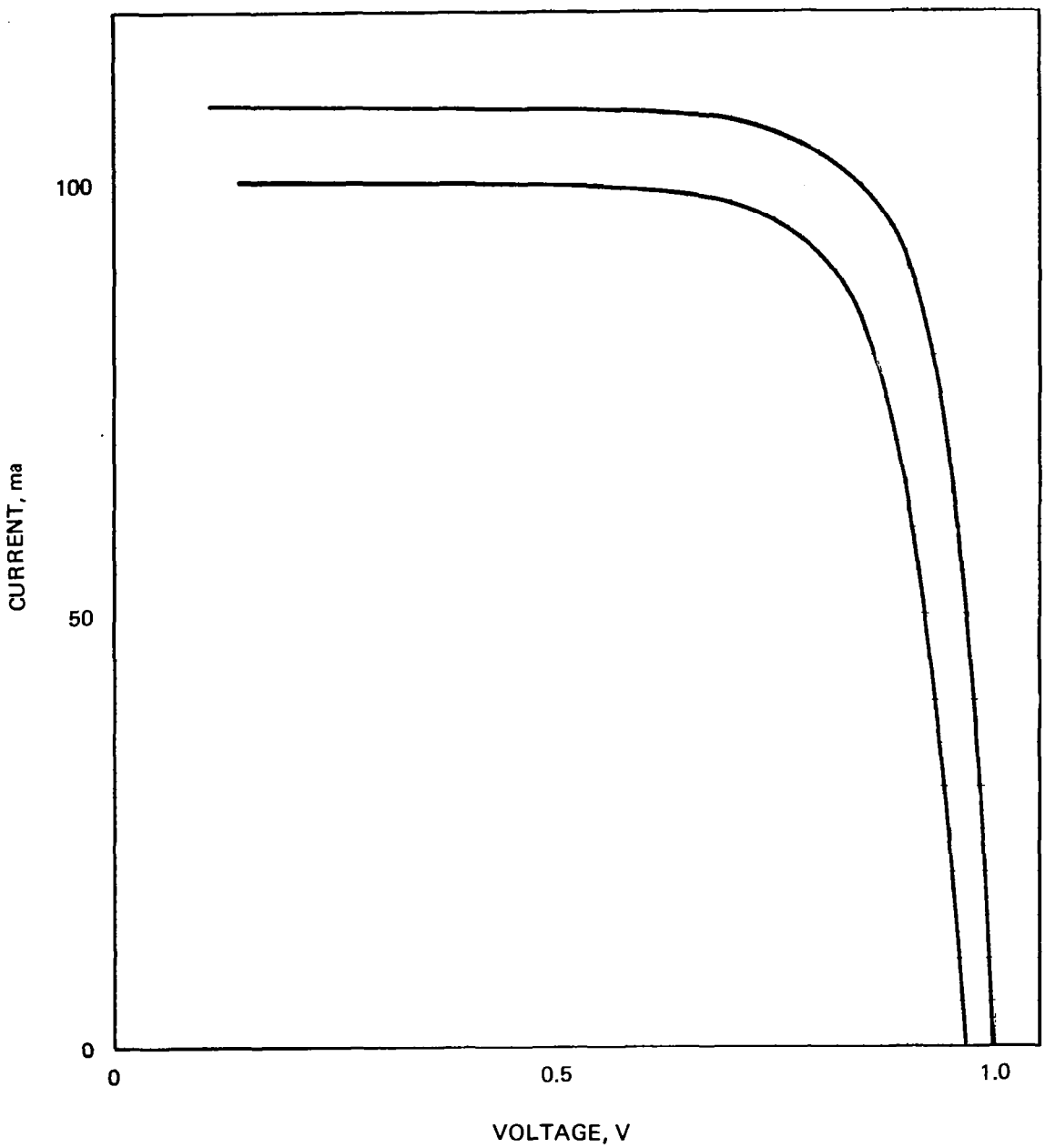

Figure 14. Photo I-V characteristics before and after proton irradiation, 40 MeV, 5 x 10^{11} P/cm^2, Cell No. 1075.

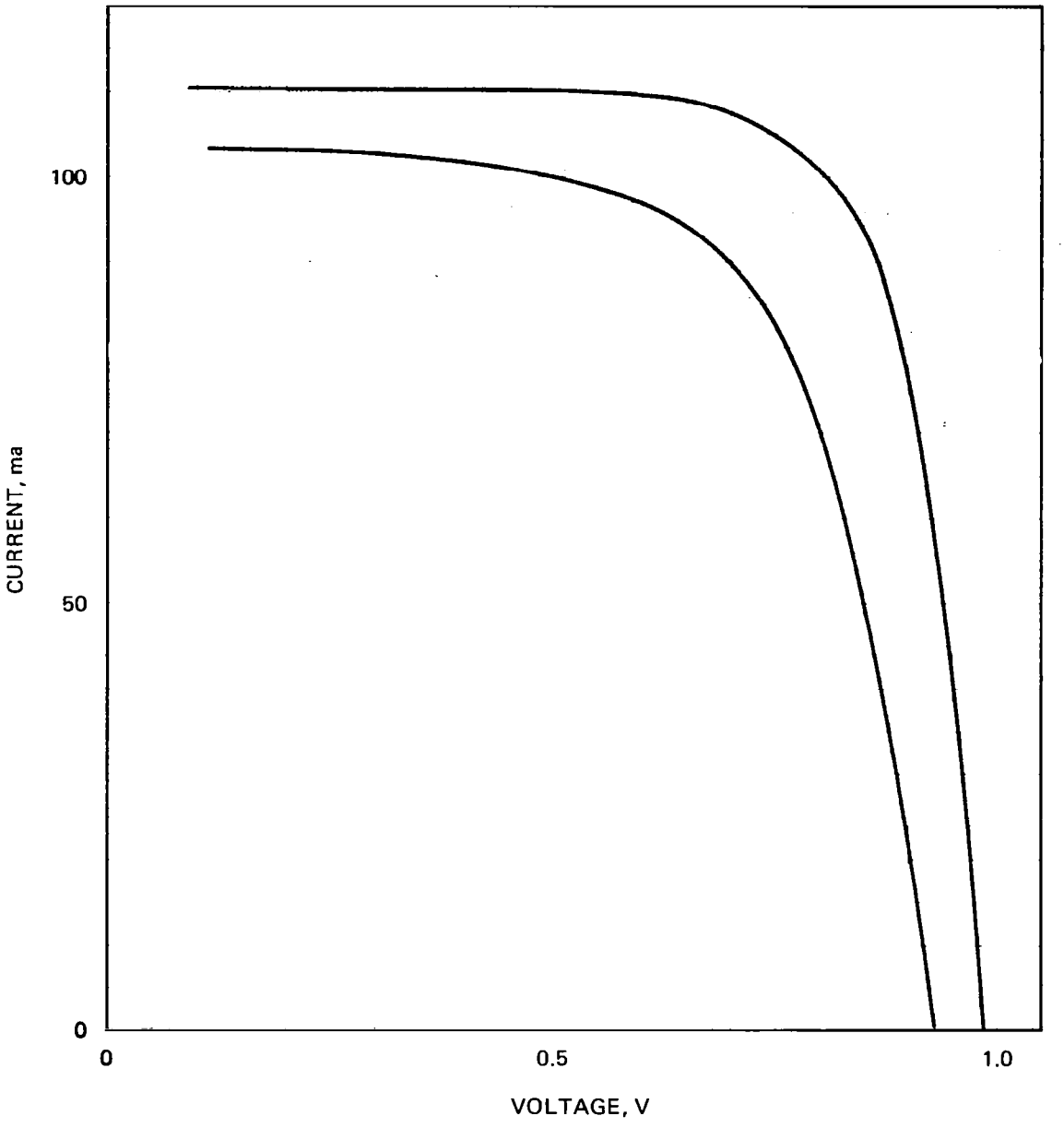

Figure 15. Photo I-V characteristics before and after proton irradiation, 40 MeV, 5 x 10^{11} P/cm^2, Cell No. 1090.

SECTION 3

SPECTRAL RESPONSE

Spectral response measurements were made on the solar cells used in the irradiation studies to give the spectral quantum efficiency of each cell. Figures 16 and 17 show the average spectral response of the (AlGa)As-GaAs solar cell before and after proton irradiation with proton energies of 15.4 MeV and 40 MeV, respectively. The spectral response in the short wavelength region of these shallow-junction solar cells is almost insensitive to the proton irradiation. A slight decrease in the solar cell spectral response occurs only in the long wavelength region. The decrease in the solar cell's spectral response after proton irradiation can be explained by the reduction of the diffusion length on both sides of the junction. Since these solar cells have shallow junctions ($x_j << L_n$), the collection of minority carriers in the p region is not affected until a critical fluence is reached when L_n is reduced to a value that is equal to or less than x_j. The degradation of hole diffusion length L_p by proton irradiation affects the minority carrier collection efficiency in the n region; this is reflected in the decrease of the spectral response in the long wavelength region. (The long wavelength light penetrates deeper into the GaAs than the shorter wavelength light.) Thus, the quality of the n buffer layer becomes increasingly important for the shallow-junction solar cells.

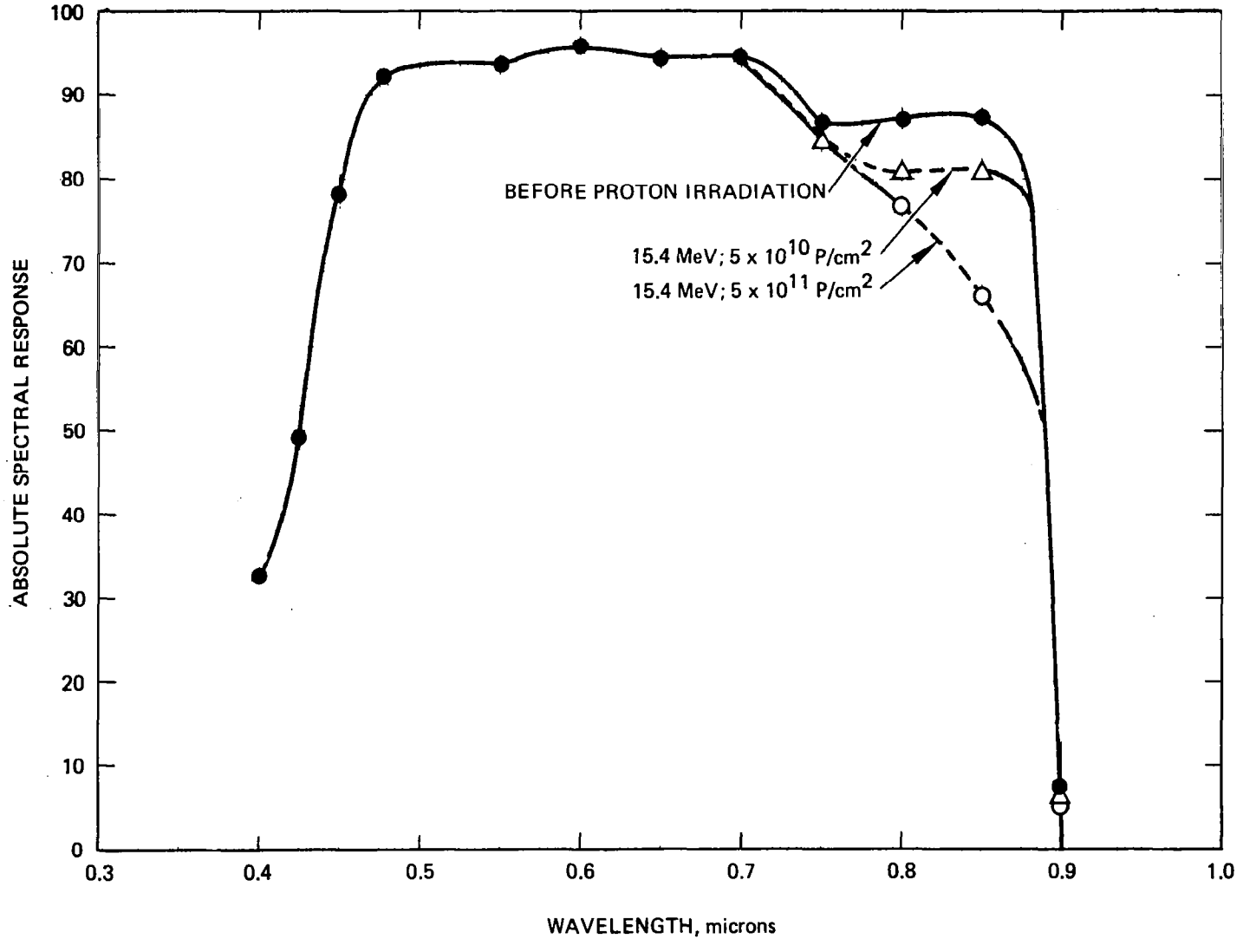

Figure 16. (AlGa)As-GaAs solar cell spectral response before and after 15.4 MeV proton irradiation.

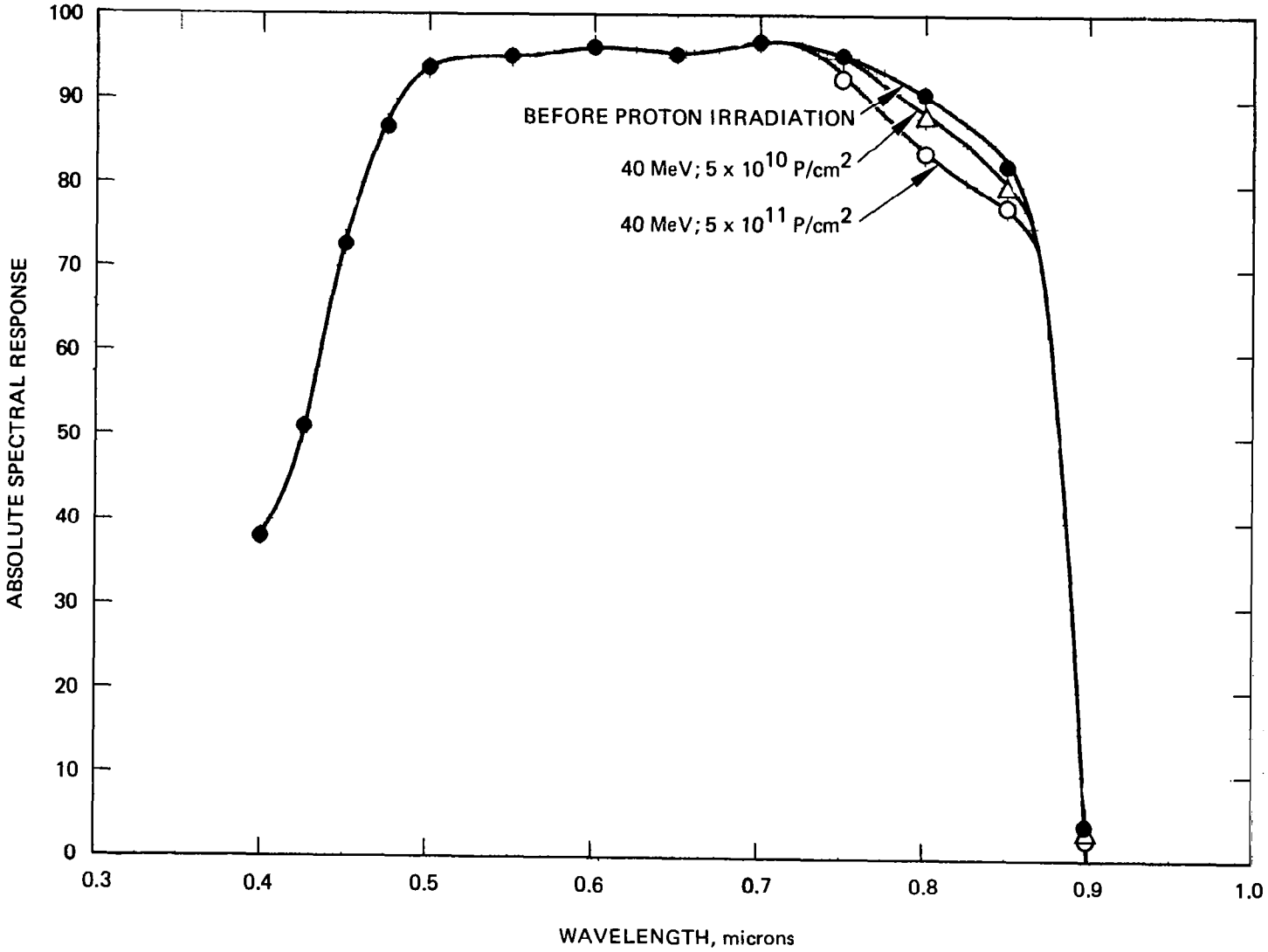

Figure 17. (AlGa)As-GaAs solar cell spectral response before and after 40 MeV proton irradiation.

SECTION 4

DIFFUSION LENGTH

When high-energy protons enter a solar cell they cause a considerable amount of lattice damage, or defects, that usually act as recombination centers and lower the minority carrier lifetimes and diffusion lengths in the cell. As a first approximation, the distribution of damage centers in the cell can be considered to be uniform, with most damage centers located far away from the junction. A convenient way of measuring the effects or the resulting loss in solar cell efficiency caused by a given particle at a given energy is to determine the degradation in the minority carrier diffusion length. The degradation of solar cells in terms of the changes in the minority carrier diffusion length can be characterized by

$$\frac{1}{L^2} = \frac{1}{L_o^2} + K_L \Phi \quad , \tag{1}$$

where L_o is the initial value of the diffusion length, L is the final value, and K_L is the damage constant (which is directly proportional to the density of recombination centers). Once the damage constants K_L and Φ are known, I_{sc}, V_{oc}, P_{max} and the output power efficiency for the cells can be calculated.

Figure 18 shows a mesa diode representation of the (AlGa)As-GaAs solar cell structure*; these mesas were used for diffusion length measurements using the electron-beam-induced current (EBIC) technique. In this technique, the beam of a scanning electron microscope (SEM) generates minority carriers near the surface of the semiconductor which diffuse towards the junction. The EBIC, I , varies exponentially with scan distance x

$$I(x) = I_o \exp\left(-\frac{X}{L}\right) \quad . \tag{2}$$

*The minority carrier diffusion length measurements were not made on the test solar cells because this is a destructive measurement. These measurements were performed on mesa diodes on pieces of material cleaved from the wafers when the cell blanks are sized to the final 2 cm x 2 cm dimensions.

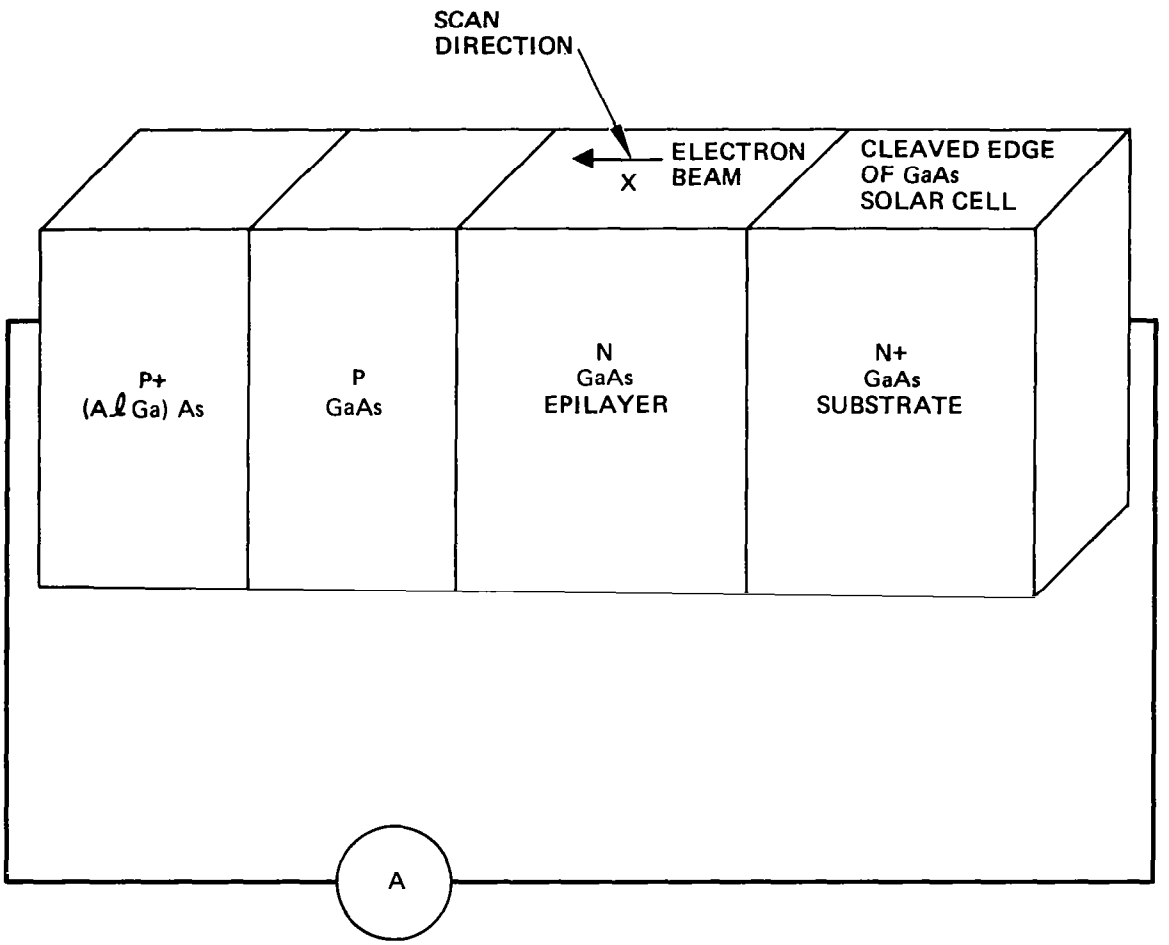

Figure 18. EBIC method of minority carrier diffusion length measurement using SEM technique.

Thus, the minority carrier diffusion length L is determined from the linear portion of the plot of log I versus x. Figure 19 shows a typical response of an experimental log I versus x curve. The shape of the curve near the junction is related to the surface and bulk recombination effect. There is only a limited straight region. Table 4 gives the measured diffusion length before and after the high-energy proton irradiation measured using this technique.

The damage constant K_L which describes the rate of change of the diffusion length with respect to the proton fluences is calculated from Eq. 1 using the measured values of diffusion length. They are 1.2×10^{-4} and 2.4×10^{-4} at 15.4 MeV and 40 MeV proton energies, respectively. However, considering the small number of samples tested and the scatter in the results, the value of K_L needs to be confirmed by a larger number of measurements.

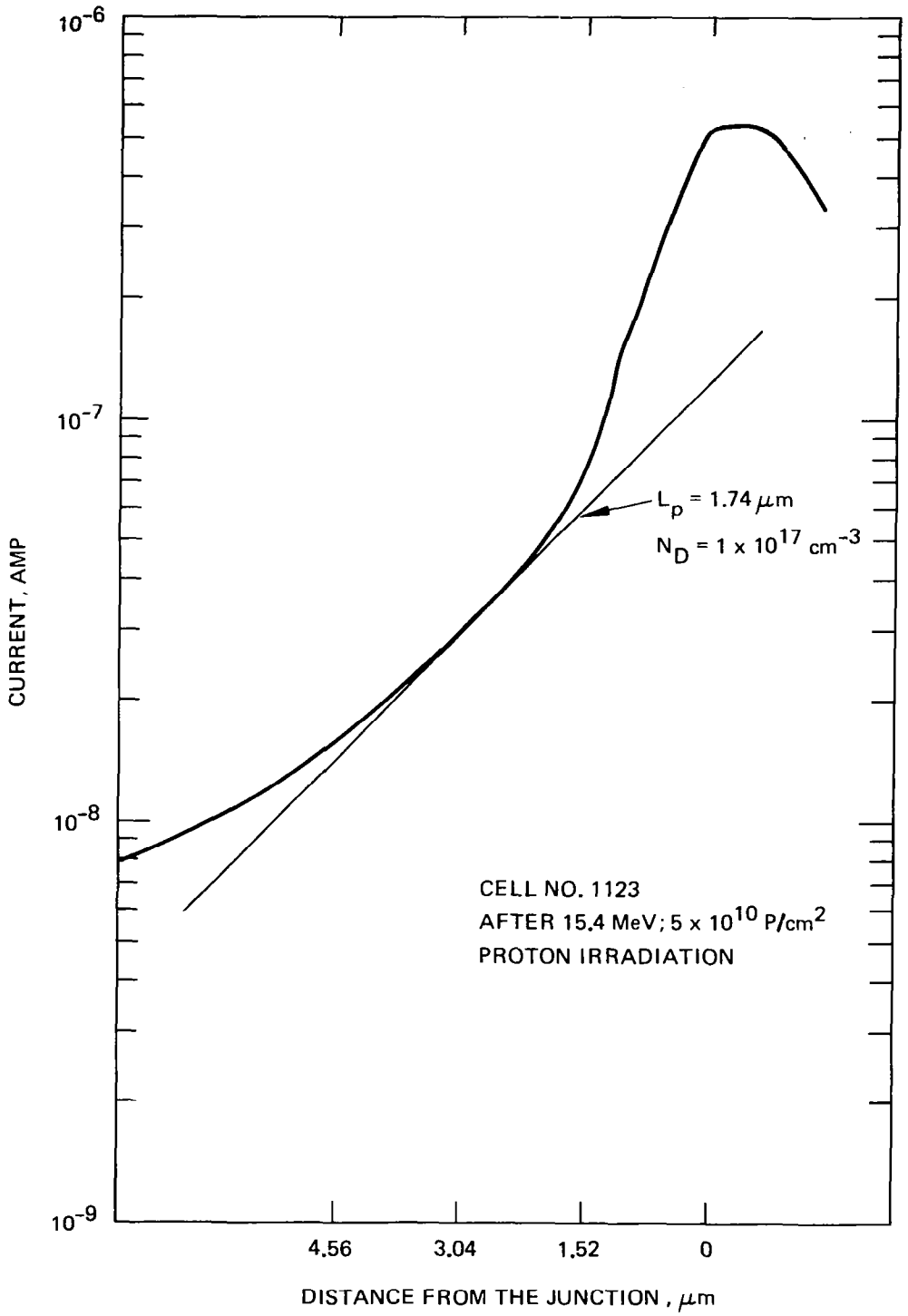

Figure 19. Electron beam induced current versus distance for (AlGa)As-GaAs solar cell (diffusion length measurement).

SECTION 5

CONCLUSIONS

This investigation has shown that the damage on (AlGa)As-GaAs solar cells in the proton energy range examined (15.4 MeV and 40 MeV) is significantly less than that for silicon cells. But a more detailed understanding of the proton damage characteristics would require covering a larger range of proton energies and fluences. The study of the influence of low-energy protons should be given special emphasis. The low-energy protons stop within the short active distance (light penetration depth) of the (AlGa)As-GaAs solar cells; they produce a relatively high amount of damage. However, the cells can be effectively shielded by a cover glass; the optimum cover glass thickness is to be determined in view of the contemplated mission.

The variation in the degradation of the power conversion efficiency in the two sets of (AlGa)As-GaAs cells indicates that these cells can be further optimized to increase their resistance to proton irradiation. The factors that control this degradation need to be analyzed in more detail.

Table 4.

Hole Diffusion Length in the (AlGa)As-GaAs Solar Cell Versus Proton Fluence

Proton Energy, MeV	Hole Diffusion Length, L_p, μm*		
15.4	3[a]	1.74[b]	1.2
40	3[a]	1.85[b]	1.24[c]

[a] Corresponds to the case before radiation

[b] Corresponds to a 5×10^{10} cm^{-2} fluence

[c] Corresponds to a 5×10^{11} cm^{-2} fluence.

* Each value of the hole diffusion length reported here is measured from one sample.

The diffusion length damage constants are found to be 1.2×10^{-4} and 2.4×10^{-4} at 15.4 MeV and 40 MeV proton energies, respectively.

For future work, it is important to make measurements at different energies and fluences. Also optimum cover glass thickness needs to be optimized to minimize degradation and establish the life expectancy of the (AlGa)As-GaAs solar cells in space for specific missions depending on the radiation spectrum they encounter during their mission life.

APPENDIX A

Representative proton fluences encountered in practical space missions are shown in Figure A-1 as a function of proton energy. The curve for cumulative solar protons is applicable to conditions encountered in synchronous orbit. The curves for elliptical and for circular equatorical orbit are representative of conditions prevalent in several missions of practical interest. These observations and inspection of Figure A-1 led to the selection of the following proton energies and fluences for the radiation damage measurements:

- Proton energies: 10 MeV* and 40 MeV
- Proton fluences: 5×10^{10} cm^{-2} and 5×10^{11} cm^{-2}.

*The experiment was intended to be a 10 MeV irradiation; however subsequent calibration tests showed the level to be 15.4 MeV instead of the 10 that was planned.

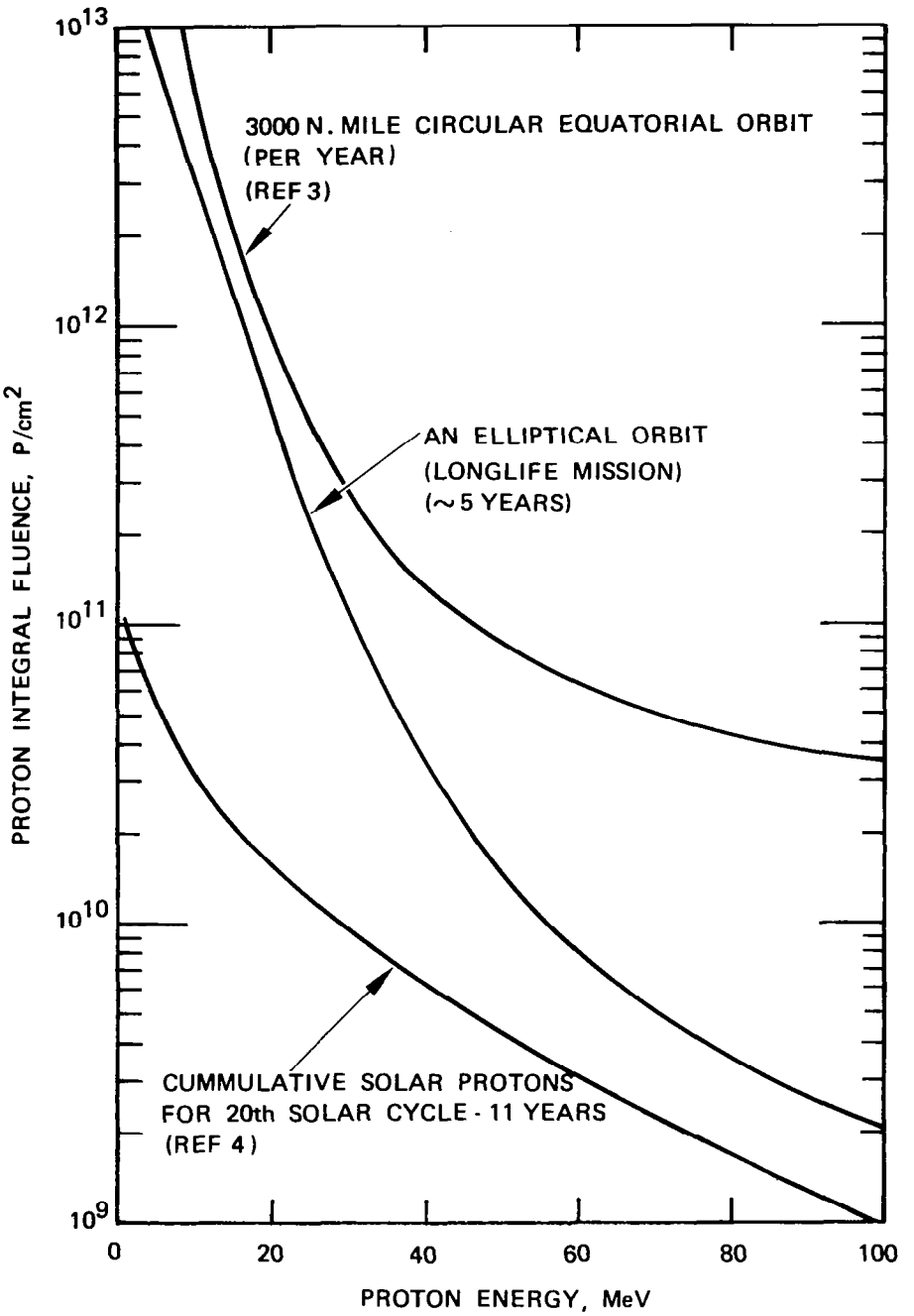

Figure A-1. Proton integral fluence as a function of proton energy.

APPENDIX B

PROTON IRRADIATION TESTS OF SILICON SOLAR CELLS

Several representative silicon solar cells (K7 qualification cells and conventional cells) were irradiated by high-energy protons together with the 12 (AlGa)As-GaAs solar cells for direct comparison. The matrix of measurements performed was given in Table 1.

The electrical characteristics for each individual K7 Si cell and conventional Si cell before and after proton irradiation are given in Tables B-1 and B-2, respectively.

Table B-1. Electrical Characteristics of K7 Bare Si Cells Before and After Proton Irradiation

Cell Number	Proton MeV	Fluence Level, p/cm^2	I_{sco}, mA	V_{oc}, V	FF	P_{max}, mW	η_o, %	$\frac{\Delta I_{sc}}{I_{sco}}$, %	$\frac{\Delta_\eta}{\eta_o}$, %
27	0	0	179.49	0.581	0.762	79.53	14.0		
	15.4	5×10^{10}	164.25	0.555	0.760	69.24	12.18	8.5	13.0
36	0	0	180.66	0.579	0.773	80.87	14.22		
	15.4	5×10^{10}	165.96	0.555	0.763	70.24	12.35	8.1	13.15
48	0	0	179.96	0.580	0.767	80.05	14.08		
	15.4	5×10^{10}	165.72	0.553	0.763	69.98	12.31	7.9	12.57
86	0	0	181.38	0.583	0.771	81.49	14.33		
	15.4	5×10^{10}	166.38	0.554	0.764	70.43	12.38	8.27	13.61
96	0	0	181.79	0.579	0.774	81.53	14.34		
	15.4	5×10^{10}	167.74	0.557	0.765	71.52	12.58	7.7	12.27
33	0	0	174.60	0.581	0.782	79.32	13.95		
	15.4	5×10^{11}	137.85	0.518	0.767	54.78	9.63	21.0	30.97
41	0	0	182.72	0.580	0.762	80.77	14.2		
	15.4	5×10^{11}	144.22	0.518	0.757	56.61	9.95	21.0	30.0
50	0	0	179.57	0.575	0.774	80.06	14.08		
	15.4	5×10^{11}	143.42	0.516	0.767	56.78	9.98	20.1	29.1
87	0	0	182.32	0.580	0.777	82.123	14.44	20.7	30.5
	15.4	5×10^{11}	144.50	0.521	0.765	57.68	10.14		
69	0	0	179.57	0.576	0.779	80.57	14.17		
	40	5×10^{10}	169.11	0.562	0.768	73.03	12.84	5.8	9.39
110	0	0	180.44	0.580	0.776	81.27	14.29		
	40	5×10^{10}	168.01	0.563	0.770	73.07	12.85	6.56	10.08
76	0	0	180.23	0.579	0.773	80.674	14.19		
	40	5×10^{11}	145.52	0.522	0.766	58.20	10.23	19.26	27.9
112	0	0	186.05	0.582	0.762	82.62	14.53		
	40	5×10^{11}	150.63	0.526	0.755	59.75	10.51	19.04	27.67

Table B-2. Electrical Characteristics of Conventional Si Bare Cells Before and After Proton Irradiation

Cell Number	Proton MeV	Fluence Level, p/cm^2	I_{sco}, mA	V_{oc}, V	FF	P_{max}, mW	η_o, %	$\frac{\Delta I_{sc}}{I_{sco}}$, %	$\frac{\Delta_\eta}{\eta_o}$, %
203	0	0	145.80	0.565	0.726	59.83	11.05		
	15.4	5×10^{10}	137.35	0.551	0.722	54.68	10.10	5.8	8.6
204	0	0	143.36	0.560	0.717	57.561	10.63		
	15.4	5×10^{10}	136.33	0.548	0.709	52.978	9.78	4.9	8.0
205	0	0	143.63	0.563	0.745	60.258	11.125		
	15.4	5×10^{10}	135.47	0.552	0.732	54.704	10.10	5.68	9.21
206	0	0	145.57	0.566	0.732	60.259	11.13		
	15.4	5×10^{10}	137.17	0.552	0.722	54.686	10.1	5.77	9.26
207	0	0	146.16	0.554	0.745	60.45	11.16		
	15.4	5×10^{11}	120.79	0.514	0.72	44.85	8.28	17.36	25.8
208	0	0	143.92	0.548	0.692	54.546	10.07		
	15.4	5×10^{11}	118.81	0.505	0.679	40.74	7.52	17.45	25.32
209	0	0	143.29	0.564	0.748	60.43	11.16		
	15.4	5×10^{11}	116.71	0.518	0.734	44.349	8.19	18.55	26.6
210	0	0	141.07	0.563	0.753	59.847	11.05		
	15.4	5×10^{11}	114.19	0.518	0.732	43.297	8.00	19.05	27.6
221	0	0	138.94	0.561	0.759	59.16	10.92		
	40	5×10^{10}	132.6	0.552	0.747	54.68	10.1	4.56	7.5
222	0	0	145.83	0.564	0.743	61.10	11.28		
	40	5×10^{10}	139.10	0.555	0.735	56.76	10.48	4.61	7.1
223	0	0	143.57	0.564	0.741	59.95	11.07		
	40	5×10^{10}	136.95	0.558	0.727	55.28	10.21	4.61	7.86
224	0	0	143.63	0.563	0.743	60.124	11.1		
	40	5×10^{11}	119.76	0.524	0.728	45.715	8.44	16.62	24.0
225	0	0	140.87	0.561	0.752	59.473	10.98		
	40	5×10^{11}	116.64	0.521	0.736	44.793	8.27	17.2	24.7
226	0	0	141.6	0.560	0.753	59.801	11.04		
	40	5×10^{11}	116.6	0.522	0.735	44.753	8.26	17.66	25.2

1. Report No.	2. Government Accession No.	3. Recipient's Catalog No.
NASA CR-3148		

4. Title and Subtitle	5. Report Date
High Energy Proton Radiation Damage to (AlGa)As—GaAs Solar Cells	June 1979
	6. Performing Organization Code
7. Author(s)	8. Performing Organization Report No.
R. Loo, L. Goldhammer, S. Kamath, and R. C. Knechtli	
	10. Work Unit No.
9. Performing Organization Name and Address	
Hughes Research Laboratories 3011 Malibu Canyon Road Malibu, California 90265	11. Contract or Grant No. NAS1-14727
	13. Type of Report and Period Covered Contractor Report Nov. 23, 1976-Oct. 15, 1977
12. Sponsoring Agency Name and Address	14. Sponsoring Agency Code
National Aeronautics and Space Administration Washington, DC 20546	

15. Supplementary Notes

Langley Technical Monitor: Gilbert H. Walker
Final Report

16. Abstract

Twelve 2 x 2 cm^2 (AlGa)As-GaAs solar cells were fabricated at Hughes Research Laboratories in Malibu and were subjected to 15.4 and 40 MeV of proton irradiation. The results show that the GaAs cells degrade considerably less than do conventional and developmental K7 silicon cells. The detailed characteristics of the GaAs and silicon cells both before and after irradiation are described. Further optimization of the GaAs cells seem feasible, and areas for future work are suggested.

17. Key Words (Suggested by Author(s))	18. Distribution Statement
Solar cells Radiation damage Proton irradiation	Unclassified - Unlimited Subject Category 33

19. Security Classif. (of this report)	20. Security Classif. (of this page)	21. No. of Pages	22. Price*
Unclassified	Unclassified	37	$4.50

* For sale by the National Technical Information Service, Springfield, Virginia 22161

NASA-Langley, 1979